Mechanics of fiber composites with fibers resistant to extension and flexure

Mahdi Zeidi and Chun IL Kim

Department of Mechanical Engineering, University of Alberta, Edmonton, Alberta, Canada

Abstract

A model of elastic solids reinforced with fibers resistant to extension and bending is formulated in finite-plane elastostatics. The linear theory of the proposed model is also derived through which a complete analytical solution is obtained. The presented model can serve as an alternative two-dimensional Cosserat theory of non-linear elasticity.

Keywords

1. Introduction

The mechanics of fiber-reinforced materials is a well-established subject [1–5] that has significantly advanced our knowledge on and practices in the development of composite materials. One way of addressing this problem is to examine the local behavior of an individual microstructure-matrix system including the interfacial region [3, 5, 6]. Such investigations are essential to extracting the mechanical properties of those materials, yet rather inefficient at predicting the general behavior of the composite materials under prescribed forces and/or displacements. Instead, one can model and formulate macroscopic behavior of the composite body in such a way that the overall contributions of microscopic responses induced by its microstructure are integrated into the models of deformations with sufficient accuracy. Within this prescription, much theoretical work has been developed based on the simple concept of an anisotropic material where the material response function depends on the classical deformation gradient with the augmented constraints of bulk incompressibility and fiber inextensibility. The resulting prediction models are often so constrained that they are not able to capture the general behavior of composites, especially those arising in fibers [7, 8]. The accommodation of fibers' mechanical responses was absent from the literature until Spencer and Soldatos [9] included bending resistance of a fiber into the model of deformations based on the non-linear strain-gradient theory [10–12]. A general theory for an elastic solid with fibers resistant to flexure, stretch and twist is presented in [13] with the special restrictions that the gradient of fiber stretch does not contribute to bending and twisting effects. In the present work, we develop a continuum model in which the fibers accommodate elastic resistance to flexure and stretch. The fibers are treated as continuously distributed spatial rods of the Kirchhoff type where the kinematics are based on their position field and a director field. The variational computation along the length of a fiber accounts for flexure while the position field provides the fiber's stretch. We seek a complete model describing the finite plane deformation of fiber

Corresponding author:
Chun IL Kim, Department of Mechanical Engineering, University of Alberta, Edmonton, Alberta T6G 2G8, Canada.
Email: cikim@ualberta.ca

composites which offers fiber resistance to extension and flexure loading. Hence, we assume that the field of the fibers' directions is a plane field, with no components in the out-of-plane direction, and where the corresponding deformation and all material properties are independent of the out-of-plane coordinate. The presented model can serve as an alternative two-dimensional Cosserat theory of non-linear elasticity [10, 14–16].

The basic kinematics and constitutive framework are presented in Section 2. Via the computation of variational derivatives and the virtual-work statement, in Section 3 the corresponding equilibrium equation is derived in which the bulk incompressibility condition is augmented in a weak sense. There we also consider an example in the case of neo-Hookean materials. With the Euler equation satisfied, in Section 4 a rigorous analysis is conducted regarding the necessary boundary conditions. To this end, we examine a special case where a composite is reinforced by a single unidirectional fiber family. A set of numerical solutions is obtained via a finite element analysis. The results are also compared with the experimental data demonstrating that the proposed model successfully predicts the deformed configuration of a crystalline nanocellulose (CNC) fiber composite subjected to three-point bending. A linear theory of the present model is discussed in Section 5. This includes the derivation of the linearized Euler equation, corresponding boundary conditions and the constraint of material incompressibility. In Section 6, a complete analytical solution of the linearized system is obtained for the case when the fiber composite is subjected to uniform bending moment at its edge.

Throughout the manuscript, we use standard notation such as $\mathbf{A}^{\mathrm{T}}$, $\mathbf{A}^{-1}$, $\mathbf{A}^*$ and $\mathrm{tr}(\mathbf{A})$. These are the transpose, the inverse, the cofactor and the trace of a tensor $\mathbf{A}$, respectively. The tensor product of vectors is indicated by interposing the symbol $\otimes$, and the Euclidean inner product of tensors $\mathbf{A}$, $\mathbf{B}$ is defined by $\mathbf{A} \cdot \mathbf{B} = \mathrm{tr}(\mathbf{AB}^{\mathrm{T}})$; the associated norm is $|\mathbf{A}| = \sqrt{\mathbf{A} \cdot \mathbf{A}}$. The symbol $|\cdot|$ is also used to denote the usual Euclidean norm of vectors. Latin and Greek indices take values in $\{1, 2\}$ and, when repeated, are summed over their ranges. Lastly, the notation $F_{\mathbf{A}}$ stands for the tensor-valued derivatives of a scalar-valued function $F(\mathbf{A})$.

2. Kinematics and constitutive framework

The present model is a special case of the work of [13] in which the author developed a model incorporating fibers resistant to twist in addition to flexure and stretch. More precisely, the suggested model is intended for the analysis of plane finite deformations of elastic solids reinforced with fibers resistant to extension and flexure. We propose that the mechanical response of the fiber material is governed by the following strain energy function:

$$W(\mathbf{F}, \mathbf{G}) = \widehat{W}(\mathbf{F}) + W(\mathbf{G}), \quad W(\mathbf{G}) \equiv \frac{1}{2} C(\mathbf{F}) |\mathbf{g}|^2, \tag{1}$$

where $\mathbf{F}$ is the gradient of the deformation function ($\chi(\mathbf{X})$) and $\mathbf{G}$ is the second gradient of the deformation (i.e. $\mathbf{G} = \nabla \mathbf{F}$). Equation (1) is consistent with the model proposed by Spencer and Soldatos [9] where, in the case of a single family of fibers, the dependence of the strain energy on $\mathbf{G}$ occurs through $\mathbf{g}$. The orientation of a particular fiber is given by

$$\lambda = |\mathbf{d}| \text{ and } \lambda \tau = \mathbf{d}; \lambda \equiv \frac{ds}{dS} \text{ and } \tau \equiv \frac{d\mathbf{r}(s)}{ds}, \tag{2}$$

where

$$\mathbf{d} = \mathbf{FD}, \tag{3}$$

in which $\mathbf{D}$ is the unit tangent to the fiber trajectory in the reference configuration. Equation (3) can be derived by taking the derivative of $\mathbf{r}(s) = \chi(\mathbf{X}(s))$ upon making the identifications $\mathbf{D} = \mathbf{X}'(s)$ and $\mathbf{d} = \mathbf{r}'(s)$. Here primes refer to derivatives with respect to arc length along a fiber in the reference configuration (i.e. $(*)' = d(*)/dS$). The expression for geodesic curvature of an arc ($\mathbf{r}(s)$) is then obtained from equation (3) as

$$\mathbf{g} \equiv \mathbf{r}'' = (\mathbf{FD})' = \mathbf{F}'\mathbf{D} + \mathbf{FD}' = \mathbf{F}'\mathbf{D} = \frac{d\mathbf{F}}{d\mathbf{X}}\left(\frac{d\mathbf{X}}{ds} \otimes \mathbf{D}\right) = \mathbf{G}(\mathbf{D} \otimes \mathbf{D}), \tag{4}$$

for initially straight fibers (i.e. $\mathbf{D}' = 0$). Also, equations (2) and (3) furnish

$$\lambda^2 = \mathbf{FD} \cdot \mathbf{FD} = \mathbf{F}^{\mathrm{T}}\mathbf{FD} \cdot \mathbf{D} = \mathbf{CD} \cdot \mathbf{D} = \mathbf{C} \cdot \mathbf{D} \otimes \mathbf{D}. \tag{5}$$

The compatibility condition of $\mathbf{F}$ can be seen as

$$G_{iAB} = F_{iA,B} = F_{iB,A} = G_{iBA}. \tag{6}$$

Let us suppose that $C(\mathbf{F}) = C$ and

$$\widehat{W}(\mathbf{F}) = W(I, \varepsilon), \text{ where } I = \text{tr}\mathbf{C} = \lambda_1^2 + \lambda_2^2 \text{and } \varepsilon = \frac{1}{2}(\lambda^2 - 1) = \frac{1}{2}(\mathbf{C} \cdot \mathbf{D} \otimes \mathbf{D} - 1). \tag{7}$$

We then have

$$W(I, \varepsilon, \mathbf{g}) = W(I, \varepsilon) + \frac{1}{2}C|\mathbf{g}|^2 = W(\mathbf{F}, \mathbf{G}). \tag{8}$$

To compute response functions $\partial W / \partial F_{iA}$ and $\partial W / \partial G_{iAB}$ for use in the Euler equation and natural boundary conditions, we use the chain rule

$$\frac{\partial W}{\partial F_{iA}}\dot{F}_{iA} + \frac{\partial W}{\partial G_{iAB}}\dot{G}_{iAB} = \dot{W}, \tag{9}$$

where the superposed dot refers to derivatives with respect to a parameter at a certain fixed value (e.g. $\epsilon = 0$) that labels a one-parameter family of deformations. Accordingly, in view of equation (8), we have that

$$\dot{W} = \dot{W}(I, \varepsilon, \mathbf{g}) = W_I \dot{I} + W_\varepsilon \dot{\varepsilon} + W_\mathbf{g} \cdot \dot{\mathbf{g}}, \tag{10}$$

in which we have used the fact that W depends on the deformation through I, ε and $\mathbf{g}$; ultimately $\mathbf{F}$ and $\mathbf{G}$. To derive the required expressions, we use (7) and derive

$$\dot{I} = [\text{tr}(\mathbf{C})]^{\cdot} = (\mathbf{I} \cdot \mathbf{C})^{\cdot} = \mathbf{I} \cdot \dot{\mathbf{C}} = 2\mathbf{F} \cdot \dot{\mathbf{F}} \tag{11}$$

and $(\lambda^2)^{\cdot} = (\mathbf{FD} \cdot \mathbf{FD})^{\cdot}$. Then

$$\dot{\varepsilon} = \lambda\dot{\lambda} = \mathbf{FD} \cdot \dot{\mathbf{FD}} = \text{tr}(\mathbf{FD} \otimes \dot{\mathbf{FD}}) = \text{tr}((\mathbf{FD} \otimes \mathbf{D})\dot{\mathbf{F}}^{\text{T}}) = \mathbf{FD} \otimes \mathbf{D} \cdot \dot{\mathbf{F}}. \tag{12}$$

Thus we obtain

$$\dot{W} = 2W_I \mathbf{F} \cdot \dot{\mathbf{F}} + W_\varepsilon \lambda\dot{\lambda} + C\mathbf{g} \cdot \dot{\mathbf{g}}$$
$$= 2W_I \mathbf{F} \cdot \dot{\mathbf{F}} + W_\varepsilon \mathbf{FD} \otimes \mathbf{D} \cdot \dot{\mathbf{F}} + C\mathbf{g} \cdot \dot{\mathbf{g}}. \tag{13}$$

But from (1)

$$\dot{W}(\mathbf{G}) = W_\mathbf{G} \cdot \dot{\mathbf{G}} \equiv (\frac{1}{2}C(\mathbf{F})|\mathbf{g}|^2)^{\cdot} = C\mathbf{g} \cdot \dot{\mathbf{g}}. \tag{14}$$

Also, invoking (4), the above yields

$$W_\mathbf{G} \cdot \dot{\mathbf{G}} = C\mathbf{g} \cdot \dot{\mathbf{g}} = \dot{\mathbf{G}} \cdot (C\mathbf{g} \otimes \mathbf{D} \otimes \mathbf{D}), \tag{15}$$

where $\dot{\mathbf{g}} = \dot{\mathbf{G}}(\mathbf{D} \otimes \mathbf{D})$, $\dot{\mathbf{D}} = 0$ for initially straight fibers. Thus we derive that

$$\frac{\partial W}{\partial G_{iAB}} = Cg_i D_A D_B. \tag{16}$$

In order to accommodate bulk incompressibility, we introduce an augmented energy potential as

$$U(I, \varepsilon, \mathbf{g}, p) = W(I, \varepsilon, \mathbf{g}) - p(J - 1). \tag{17}$$

Then

$$\dot{U} = \dot{W} - \dot{p}(J - 1) - p\dot{J} = \dot{W} - p\dot{J}, \quad \because \dot{p}(J - 1) = 0 \text{ for } J = 1. \tag{18}$$

Further, since $\dot{J} = \frac{\partial J}{\partial \mathbf{F}} \cdot \dot{\mathbf{F}} = J(\mathbf{F}^{-1})^{\text{T}} \cdot \dot{\mathbf{F}} = \mathbf{F}^* \cdot \dot{\mathbf{F}}$, combining (13) and (18) furnishes

$$\dot{U} = 2W_I \mathbf{F} \cdot \dot{\mathbf{F}} + W_\varepsilon \mathbf{FD} \otimes \mathbf{D} \cdot \dot{\mathbf{F}} - p\mathbf{F}^* \cdot \dot{\mathbf{F}} + C\mathbf{g} \cdot \dot{\mathbf{g}}. \tag{19}$$

Consequently, from (14), the above can be written as

$$\dot{U} = (2W_I \mathbf{F} + W_\varepsilon \mathbf{FD} \otimes \mathbf{D} - p\mathbf{F}^*) \cdot \dot{\mathbf{F}} + W_\mathbf{G} \cdot \dot{\mathbf{G}}, \tag{20}$$

in which we have imposed fibers resistant to extension, flexure and the requisite bulk incompressibility.

3. Equilibrium

The derivation of the Euler equation and boundary conditions in second-gradient elasticity is well studied [10–12, 17]. We reproduce it here for the sake of clarity and completeness of the proposed model, in particular the connections between the applied loads and the deformations. The weak form of the equations of equilibrium is given by the virtual-work statement

$$\dot{E} = P, \tag{21}$$

where P is the virtual work of the applied loads and the superposed dot refers to the variational derivative;

$$E = \int_{\Omega} U(\mathbf{F}, \mathbf{G}) \, dA \tag{22}$$

is the strain energy. We note here that conservative loads are characterized by the existence of a potential L such that $P = \dot{L}$, and in the present case the problem of determining equilibrium deformations is reduced to the problem of minimizing the potential energy $E - L$.

We have

$$\dot{E} = \int_{\Omega} \dot{U}(\mathbf{F}, \mathbf{G}) \, dA, \tag{23}$$

where $\dot{U}$ is given by (20). Writing

$$W_{\mathbf{G}} \cdot \dot{\mathbf{G}} = \frac{\partial W}{\partial G_{iAB}} \dot{G}_{iAB} = \frac{\partial W}{\partial G_{iAB}} \dot{F}_{iA,B} = \frac{\partial W}{\partial G_{iAB}} u_{i,AB}; \ u_i \equiv \dot{r}_i = \dot{\chi}_i, \text{ and}$$

$$\frac{\partial W}{\partial G_{iAB}} u_{i,AB} = \left(\frac{\partial W}{\partial G_{iAB}} u_{i,A} \right)_{,B} - \left(\frac{\partial W}{\partial G_{iAB}} \right)_{,B} u_{i,A}, \tag{24}$$

we obtain

$$\int_{\Omega} W_{\mathbf{G}} \cdot \dot{\mathbf{G}} \, dA = \int_{\Omega} \left(\frac{\partial W}{\partial G_{iAB}} u_{i,A} \right)_{,B} dA - \int_{\Omega} \left(\frac{\partial W}{\partial G_{iAB}} \right)_{,B} u_{i,A} \, dA. \tag{25}$$

By virtue of the Green–Stokes theorem, (25) can be rewritten as

$$\int W_{\mathbf{G}} \cdot \dot{\mathbf{G}} \, dA = \int_{\partial \Omega} \frac{\partial W}{\partial G_{iAB}} u_{i,A} N_B \, dS - \int_{\Omega} \left(\frac{\partial W}{\partial G_{iAB}} \right)_{,B} u_{i,A} \, dA, \tag{26}$$

where $\mathbf{N}$ is the rightward unit normal to $\partial \Omega$. In addition, from (15)

$$\int W_{\mathbf{G}} \cdot \dot{\mathbf{G}} \, dA = \int \frac{\partial W}{\partial G_{iAB}} u_{i,A} N_B \, dS - \int C g_{i,B} D_A D_B \dot{F}_{iA} \, dA$$

$$= - \int_{\Omega} C \nabla \mathbf{g} (\mathbf{D} \otimes \mathbf{D}) \cdot \dot{\mathbf{F}} \, dA + \int_{\partial \Omega} W_{\mathbf{G}}^{\mathrm{T}} [\dot{\mathbf{F}}]^{\mathrm{T}} \cdot \mathbf{N} \, dS. \tag{27}$$

By combining (20), (23), and (27), we write

$$\dot{E} = \int_{\Omega} \mathbf{P} \cdot \dot{\mathbf{F}} \, dA + \int_{\partial \Omega} W_{\mathbf{G}}^{\mathrm{T}} [\dot{\mathbf{F}}]^{\mathrm{T}} \cdot \mathbf{N} \, dS, \tag{28}$$

where

$$\mathbf{P} = 2 W_I \mathbf{F} + W_{\varepsilon} \mathbf{F} (\mathbf{D} \otimes \mathbf{D}) - p \mathbf{F}^* - C \nabla \mathbf{g} (\mathbf{D} \otimes \mathbf{D}), \tag{29}$$

and hence the Euler equation

$$\mathrm{Div}(\mathbf{P}) = 0, \tag{30}$$

which holds in Ω.

3.1. Example: Neo-Hookean-type materials

In the case of incompressible neo-Hookean-type materials with augmented extensibility, the energy density function can be expressed as

$$W = \mu I + \frac{1}{2}E\varepsilon^2. \tag{31}$$

Thus (5), (7) and (29) yield

$$\mathbf{P} = 2\mu\mathbf{F} + \frac{1}{2}E(\mathbf{FD} \cdot \mathbf{FD} - 1)\mathbf{F}(\mathbf{D} \otimes \mathbf{D}) - p\mathbf{F}^* - C\nabla\mathbf{g}(\mathbf{D} \otimes \mathbf{D}), \tag{32}$$

and the corresponding Euler equation is obtained as

$$P_{iA,A} = 2\mu F_{iA,A} + \frac{1}{2}E(F_{iB,A}F_{jC}F_{jD} + F_{iB}F_{jC,A}F_{jD} + F_{iB}F_{jC}F_{jD,A})D_A D_B D_C D_D$$

$$-\frac{1}{2}EF_{iB,A}D_A D_B - p_{,A}F_{iA}^* - Cg_{i,AB}D_A D_B = 0. \tag{33}$$

If a fiber-reinforced material consists of a single family of fibers (i.e. $\mathbf{D} = \mathbf{E}_1$, $D_1 = 1$, $D_2 = 0$) and is subjected to plane deformations, (33) further reduces to

$$P_{iA,A} = 2\mu F_{iA,A} + \frac{1}{2}E(F_{i1,1}F_{j1}F_{j1} + F_{i1}F_{j1,1}F_{j1} + F_{i1}F_{j1}F_{j1,1})$$

$$-\frac{1}{2}EF_{i1,1} - p_{,A}F_{iA}^* - Cg_{i,11} = 0 \text{ for } i, A = 1, 2, \tag{34}$$

and

$$g_i = F_{i1,1}, \ F_{iA} = \frac{\partial \chi_i}{\partial X_A} \text{ and } F_{iA}^* = \varepsilon_{ij}\varepsilon_{AB}F_{jB}, \tag{35}$$

where ε_{ij} is the two-dimensional permutation; $\varepsilon_{12} = -\varepsilon_{21} = 1$, $\varepsilon_{11} = -\varepsilon_{22} = 0$. Therefore, equation (35) together with the incompressibility condition (det $\mathbf{F} = 1$) furnishes a coupled partial differential equation (PDE) system solving for χ_1, χ_2 and p (see appendix for details), that is,

$$2\mu(\chi_{1,11} + \chi_{1,22}) - p_{,1}\chi_{2,2} + p_{,2}\chi_{2,1} - C\chi_{1,1111} - \frac{1}{2}E\chi_{1,11}$$

$$+\frac{1}{2}E(3\chi_{1,11}\chi_{1,1}\chi_{1,1} + \chi_{1,11}\chi_{2,1}\chi_{2,1} + 2\chi_{2,11}\chi_{1,1}\chi_{2,1}) = 0,$$

$$2\mu(\chi_{2,11} + \chi_{2,22}) - p_{,2}\chi_{1,1} + p_{,1}\chi_{1,2} - C\chi_{2,1111} - \frac{1}{2}E\chi_{2,11}$$

$$+\frac{1}{2}E(3\chi_{2,11}\chi_{2,1}\chi_{2,1} + \chi_{2,11}\chi_{1,1}\chi_{1,1} + 2\chi_{1,11}\chi_{2,1}\chi_{1,1}) = 0,$$

$$\chi_{1,1}\chi_{2,2} - \chi_{1,2}\chi_{2,1} = 1. \tag{36}$$

The numerical solution of the above PDE can be obtained via commercial packages (e.g. Matlab, COMSOL, etc.). For demonstration purposes, a set of numerical solutions is obtained for a rectangular composite reinforced with a single family of fibers (unidirectional) subjected to uniform bending and/or extension (see Figures 1–5).

We note here that data are obtained under the normalized setting (e.g. $\frac{C}{\mu} = 150$, $\frac{E}{\mu} = 100$, $\frac{M}{\mu} = 5[L]^3$, etc.). A comparison with experimental results is also presented when a CNC fiber composite ($C = 150$ GPa, $\mu = 1$ GPa) is subjected to three-point bending at -10 mm, 0 mm, and 10 mm. In the test, the out-of-plane direction (x_3) is aligned with the loading cylinder (see Figure 6). This is a special case of the proposed model, when $c \gg d$ and $C/\mu = 150$ with vanishing E. The results successfully predict the normal deflections and the corresponding deformation profiles of the CNC composite strip with configuration factor $\gamma = 0.526[L]^2$ between the applied load and input stress in each simulation (i.e. $\sigma_{\text{input}} \times \gamma = \text{Load}_{\text{applied}}$; see Figures 7 and 8). In particular, Figure 7 illustrates a direct comparison with the bending experiment at maximum deflection 2.55 mm. Despite inevitable uncertainties (e.g. image processing and curve fitting, etc.), the resulting deformation profiles from both the experiment and the theoretical simulation demonstrate close correspondence throughout the domain of interest.
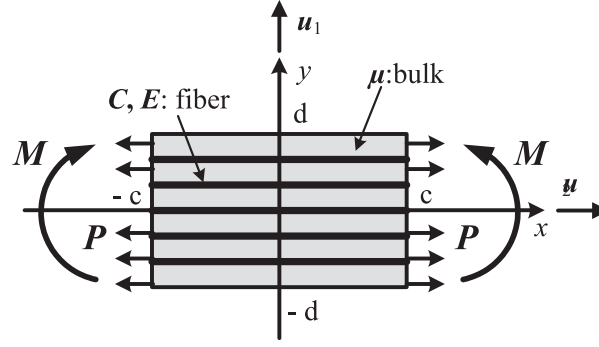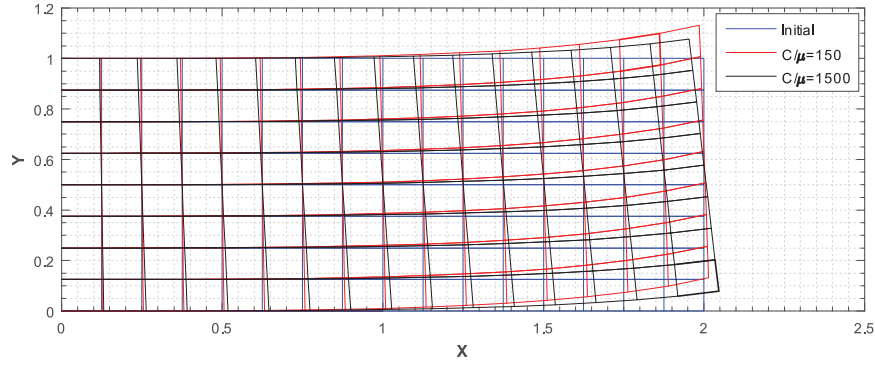
Figure 1. Schematic of problem.

Figure 2. Deformed configurations with respect to C/μ when $M/\mu = 10$, $E/\mu = 100$.
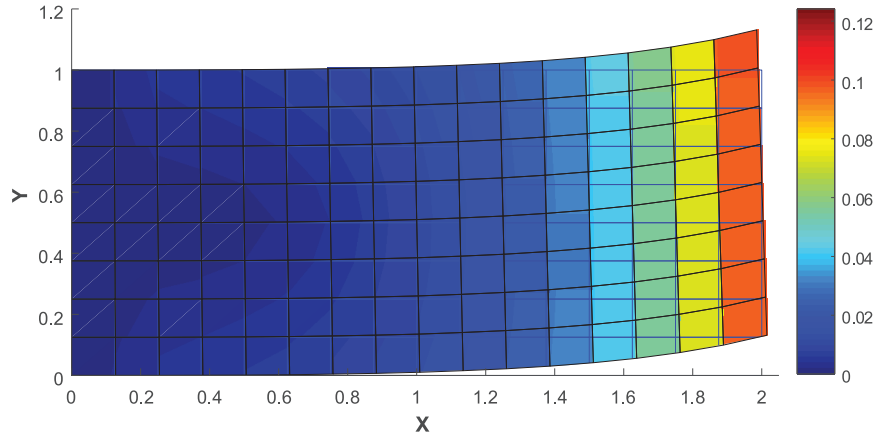

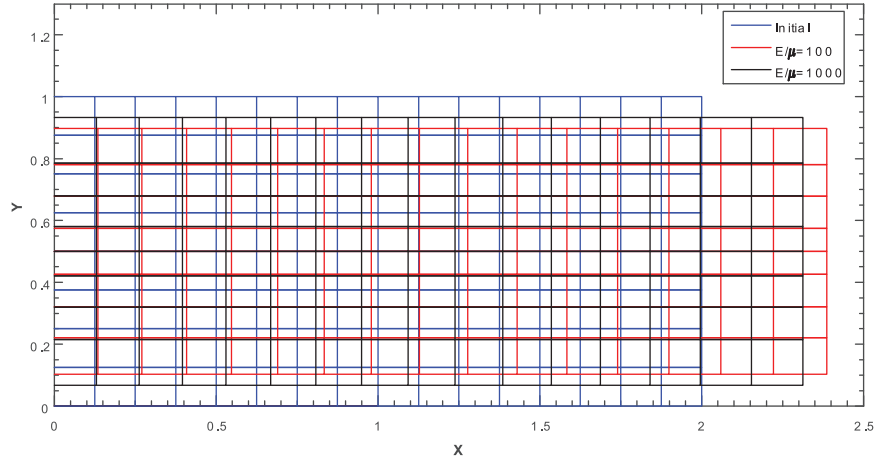**Figure 3.** Deformed contour ($\sqrt{\chi_1^2 + \chi_2^2}$) when $C/\mu = 150$, $E/\mu = 100$ and $M/\mu = 10$.
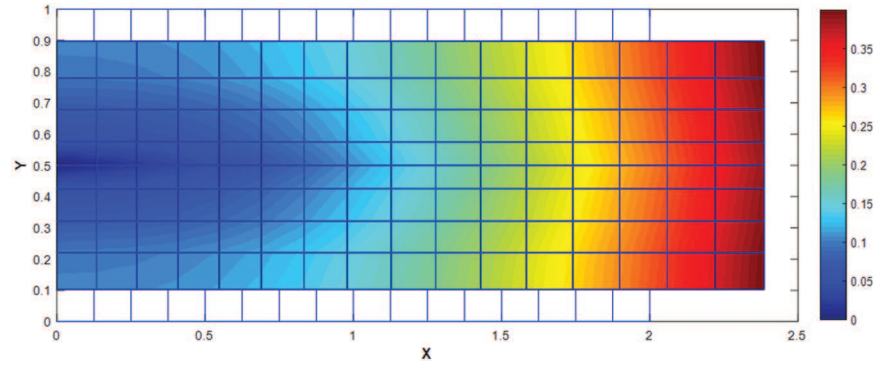
4. Boundary conditions

From (28), we have

$$\dot{E} = \int_\Omega P_{iA}\dot{F}_{iA}\, dA + \int_{\partial\Omega} \frac{\partial W}{\partial G_{iAB}}\dot{F}_{iA}N_B\, dS.$$

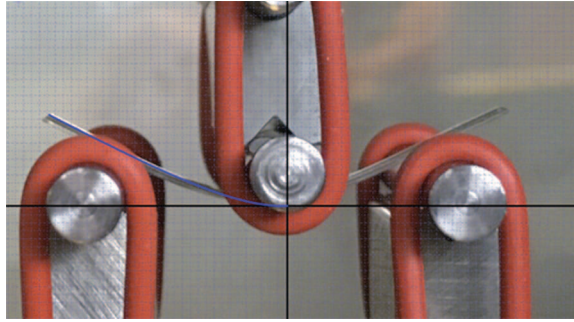Decomposing the above as in (24) furnishes

$$\dot{E} = \int_{\partial\Omega}[P_{iA}u_i N_A + \left(\frac{\partial W}{\partial G_{iAB}}u_{i,A}\right)N_B]\, dS - \int_\Omega P_{iA,A}u_i\, dA. \tag{37}$$

Figure 4. Deformed configurations with respect to E/μ when $C/\mu = 150$, $P_{11}/\mu = 50$.

Figure 5. Deformation contour ($\sqrt{\chi_1^2 + \chi_2^2}$) when $C/\mu = 150$, $E/\mu = 100$ and $P_{11}/\mu = 50$.
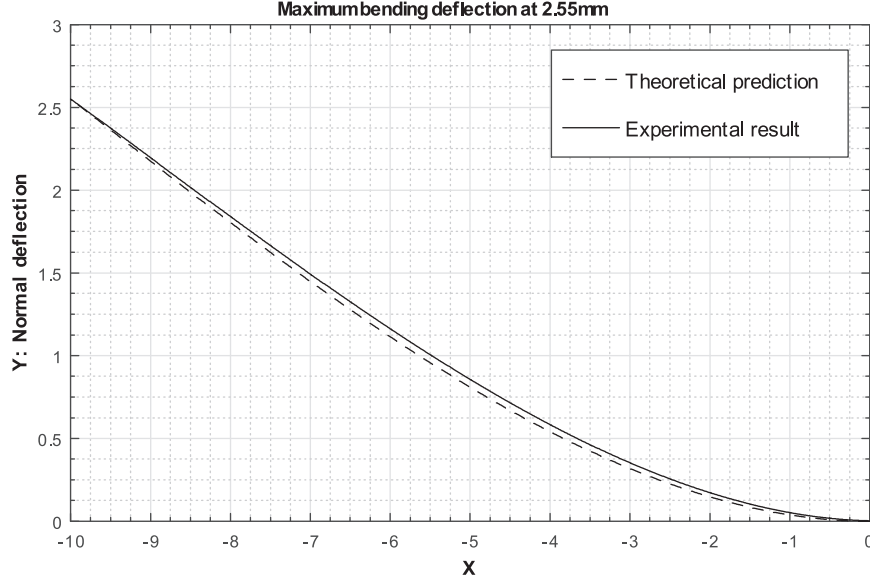

Figure 6. Deformation profile (image processing) at 2.55 mm: CNC fiber composite.

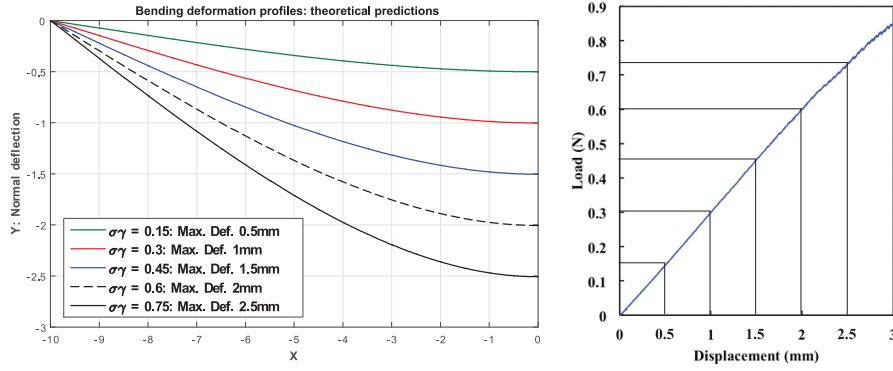With the Euler equation ($P_{iA,A} = 0$) satisfied on Ω, we have

$$\dot{E} = \int_{\partial\Omega} P_{iA} u_i N_A \, dS + \int_{\partial\Omega} \left(\frac{\partial W}{\partial G_{iAB}} u_{i,A} \right) N_B \, dS. \tag{38}$$

Now, we make use of the normal–tangent decomposition of $\nabla \mathbf{u}$ as

$$\nabla \mathbf{u} = \nabla \mathbf{u} (\mathbf{T} \otimes \mathbf{T}) + \nabla \mathbf{u} (\mathbf{N} \otimes \mathbf{N}) = \mathbf{u}' \otimes \mathbf{T} + \mathbf{u}_{,\mathbf{N}} \otimes \mathbf{N} \tag{39}$$

Figure 7. Comparison: Theoretical prediction vs experimental result at 2.55 mm.

Figure 8. Deformation profiles with respect to $\sigma\gamma$: Theoretical prediction and three-point bending experiment.

where $\mathbf{T} = \mathbf{X}'(s) = \mathbf{k} \times \mathbf{N}$ is the unit tangent to ∂w, and $\mathbf{u}' = d\mathbf{u}(\mathbf{X}(s))/ds$ and $\mathbf{u}_{,N}$ are the tangential and normal derivatives of $\mathbf{u}$ on ∂w (i.e. $u'_i = u_{i,A}T_A$, $u_{i,N} = u_{i,A}N_A$). Then, equation (38) can be rewritten as

$$\dot{E} = \int_{\partial\Omega} P_{iA}u_iN_A \, dS + \int_{\partial\Omega} \frac{\partial W}{\partial G_{iAB}} \left(u'_i T_A N_B + u_{i,N}N_A N_B \right) \, dS. \tag{40}$$

Since

$$\frac{\partial W}{\partial G_{iAB}}T_A N_B u'_i = \left(\frac{\partial W}{\partial G_{iAB}}T_A N_B u_i \right)' - \left(\frac{\partial W}{\partial G_{iAB}}T_A N_B \right)' u_i,$$

we arrive at

$$\dot{E} = \int_{\partial\Omega} [P_{iA}N_A - \left(\frac{\partial W}{\partial G_{iAB}}T_A N_B \right)']u_i \, dS + \int_{\partial\Omega} \frac{\partial W}{\partial G_{iAB}}u_{i,N}N_A N_B \, dS + \int_{\partial\Omega} \left(\frac{\partial W}{\partial G_{iAB}}T_A N_B u_i \right)' \, dS. \tag{41}$$

With the results in (16), the above becomes

$$\dot{E} = \int_{\partial\Omega} \left\{ P_{iA}N_A - (Cg_i D_A T_A D_B N_B)' \right\} u_i \, dS + \int_{\partial\Omega} Cg_i D_A N_A D_B N_B u_{i,N} \, dS - \sum \| Cg_i D_A T_A D_B N_B u_i \|, \tag{42}$$

where the double bar symbol refers to the jump across the discontinuities on the boundary $\partial\Omega$ (i.e. $\|*\| = (*)^+ - (*)^-$) and the sum refers to the collection of all discontinuities.

It follows from (21) that admissible powers are of the form

$$P = \int_{\partial w_t} t_i u_i \, dS + \int_{\partial w} m_i u_{i,N} \, dS + \sum f_i u_i. \tag{43}$$

By comparing (42) and (43), we obtain

$$\mathbf{t} = \mathbf{PN} - \frac{d}{ds}\left[C\mathbf{g}(\mathbf{D}\cdot\mathbf{T})(\mathbf{D}\cdot\mathbf{N})\right],$$
$$\mathbf{m} = C\mathbf{g}(\mathbf{D}\cdot\mathbf{N})^2,$$
$$\mathbf{f} = C\mathbf{g}(\mathbf{D}\cdot\mathbf{T})(\mathbf{D}\cdot\mathbf{N}), \tag{44}$$

which are expressions for the edge tractions, the edge moments and the corner forces, respectively. For example, if the fibers' directions are either normal or tangential to the boundary (i.e. $(\mathbf{D}\cdot\mathbf{T})(\mathbf{D}\cdot\mathbf{N}) = 0$), (44) further reduces to

$$t_i = P_{iA}N_A,$$
$$m_i = Cg_i D_A N_A D_B N_B,$$
$$f_i = 0, \tag{45}$$

where

$$P_{iA} = 2\mu F_{iA} + \frac{1}{2}E(F_{jC}F_{jD}D_C D_D - 1)(F_{iB}D_B D_A) - pF_{iA}^* - Cg_{i,B}D_B D_A,$$
$$g_i = F_{iA,B}D_A D_B. \tag{46}$$

5. Linear theory

We consider superposed "small" deformations as

$$\chi = \chi_o + \varepsilon\dot{\chi}; |\varepsilon| \ll 1, \tag{47}$$

where $(*)_o$ denotes configuration of $*$ evaluated at $\varepsilon = 0$ and $(\dot{*}) = \partial(*)/\partial\varepsilon$. (Not to be confused with the notation adopted for the variational computation.) In particular, we denote $\dot{\chi} = \mathbf{u}$. Then, the deformation gradient tensor can be written as

$$\mathbf{F} = \mathbf{F}_o + \varepsilon\nabla\mathbf{u}, \text{ where } \dot{\mathbf{F}} = \nabla\mathbf{u}. \tag{48}$$

We assume that the body is initially undeformed and stress-free at $\varepsilon = 0$ (i.e. $\mathbf{F}_o = \mathbf{I}$ and $\mathbf{P}_o = \mathbf{0}$). Then, equation (48) becomes

$$\mathbf{F} = \mathbf{I} + \varepsilon\nabla\mathbf{u}, \tag{49}$$

and we successively obtain

$$\mathbf{F}^{-1} = \mathbf{I} - \varepsilon\nabla\mathbf{u} + o(\varepsilon), \tag{50}$$

$$J = \det\mathbf{F} = 1 + \varepsilon\,\mathrm{div}\,\mathbf{u} + o(\varepsilon). \tag{51}$$

Further, in view of equation (47), equation (30) can be rewritten as

$$\mathrm{Div}(\mathbf{P}) = \mathrm{Div}(\mathbf{P}_o) + \varepsilon\mathrm{Div}(\dot{\mathbf{P}}) + o(\varepsilon) = \mathbf{0}. \tag{52}$$

Dividing the above by ε and letting $\varepsilon \to 0$, we obtain

$$\mathrm{Div}(\dot{\mathbf{P}}) = 0 \tag{53}$$

which serves as the linearized Euler equation. Now, from equation (29), we evaluate the variation of $\mathbf{P}$ with respect to ε as

$$\dot{\mathbf{P}} = 2(W_{II}\dot{I} + W_{I\varepsilon}\dot{\varepsilon})\mathbf{F}_o + 2(W_I)_o\dot{\mathbf{F}} - \dot{p}\mathbf{F}_o^* - p_o\dot{\mathbf{F}}^*$$
$$+[(W_{\varepsilon\varepsilon}\dot{\varepsilon} + W_{\varepsilon I}\dot{I})\mathbf{F}_o + (W_\varepsilon)_o\dot{\mathbf{F}} - C\nabla\dot{\mathbf{g}}](\mathbf{D} \otimes \mathbf{D}). \tag{54}$$

In view of (31), the above further reduces to

$$\dot{\mathbf{P}} = 2\mu\dot{\mathbf{F}} - \dot{p}\mathbf{F}_o^* - p_o\dot{\mathbf{F}}^* + [E\dot{\varepsilon}\mathbf{F}_o + E\varepsilon_o\dot{\mathbf{F}} - C\nabla\dot{\mathbf{g}}](\mathbf{D} \otimes \mathbf{D}). \tag{55}$$

Evaluating limits at $\varepsilon = 0$ yields

$$\dot{\mathbf{P}} = 2\mu\dot{\mathbf{F}} - \dot{p}\mathbf{I} - p_o\dot{\mathbf{F}}^* + [E\dot{\varepsilon}\mathbf{I} - C\nabla\dot{\mathbf{g}}](\mathbf{D} \otimes \mathbf{D}), \tag{56}$$

where $p_o = 2\mu$ to recover the initial stress-free state at $\varepsilon = 0$. Thus, equations (12), (53) and (56) furnish

$$\dot{p}_{,i}\mathbf{e}_i = 2\mu\dot{F}_{iA,A}\mathbf{e}_i + E\dot{F}_{jA,B}D_AD_BD_iD_j\mathbf{e}_i - C\dot{F}_{iA,BCD}D_AD_BD_CD_D\mathbf{e}_i. \tag{57}$$

We note that, in the superposed incremental deformations, there is no clear distinction between the current and deformed configurations (i.e. $\mathbf{e}_\alpha = \mathbf{E}_\alpha$). For a single family of fibers (i.e. $\mathbf{D} = \mathbf{E}_1$, $D_1 = 1$, $D_2 = 0$), (57) reduces to

$$\dot{p}_{,i}\mathbf{e}_i = 2\mu u_{i,AA}\mathbf{e}_i + Eu_{1,11}\mathbf{e}_1 - Cu_{i,1111}\mathbf{e}_i. \tag{58}$$

In addition, the corresponding incompressibility condition reduces to

$$(J - 1)^{\cdot} = \mathbf{F}_o^* \cdot \dot{\mathbf{F}} = \operatorname{div}\mathbf{u} = \mathbf{0}, \tag{59}$$

which, together with equation (58), serves as a compatible linear model of equation (36) for small deformations.

Finally, the boundary conditions in equation (44) can be linearized similarly to the above (e.g. $\mathbf{t} = \mathbf{t}_o + \varepsilon\dot{\mathbf{t}} + o(e)$, etc.):

$$\dot{\mathbf{t}} = \dot{\mathbf{P}}\mathbf{N} - \frac{d}{ds}\left[C\dot{\mathbf{g}}(\mathbf{D} \cdot \mathbf{T})(\mathbf{D} \cdot \mathbf{N})\right],$$
$$\dot{\mathbf{m}} = C\dot{\mathbf{g}}(\mathbf{D} \cdot \mathbf{N})^2,$$
$$\dot{\mathbf{f}} = C\dot{\mathbf{g}}(\mathbf{D} \cdot \mathbf{T})(\mathbf{D} \cdot \mathbf{N}). \tag{60}$$

In particular, if the fiber's directions are either normal or tangential to the boundary (i.e. $(\mathbf{D} \cdot \mathbf{T})(\mathbf{D} \cdot \mathbf{N}) = 0$), equation (60) further reduces to

$$\dot{t}_i = \dot{P}_{iA}N_A,$$
$$\dot{m}_i = C\dot{g}_iD_AN_AD_BN_B,$$
$$\dot{f}_i = 0, \tag{61}$$

and

$$\dot{P}_{iA} = 2\mu\dot{F}_{iA} - \dot{p}\delta_{iA} - p_o\dot{F}_{iA}^* + E\dot{F}_{jB}D_AD_BD_iD_j - C\dot{g}_{i,B}D_AD_B, \tag{62}$$

where $\dot{g}_i = \dot{F}_{iA,B}D_AD_B$ and $(F_{iA}^*)_o = \delta_{iA}$. Lastly, since $J\partial F_{jB}^*/\partial F_{iA} = F_{jB}^*F_{iA}^* - F_{iB}^*F_{jA}^*$ at $\mathbf{F}_o = \mathbf{I}$ we obtain

$$(\partial F_{jB}^*/\partial F_{iA})_o = \delta_{jB}\delta_{iA} - \delta_{iB}\delta_{jA} \text{ and } (\mathbf{F}_{\mathbf{F}}^*[\dot{\mathbf{F}}])_{jB} = (\delta_{jB}\delta_{iA} - \delta_{iB}\delta_{jA})u_{i,A}. \tag{63}$$

Thus

$$\dot{F}_{iA}^* = (\operatorname{Div}\mathbf{u})\delta_{iA} - u_{A,i} = -u_{A,i}, \tag{64}$$

where $\operatorname{Div}\mathbf{u} = \operatorname{div}\mathbf{u} = 0$ from the linearized incompressibility condition.

6. Solution to the linearized equation

We introduce scalar field ϕ as

$$\mathbf{u} = \mathbf{k} \times \nabla\phi, \quad \mathbf{k}(\text{unit normal}); \quad u_i = \varepsilon_{\lambda i}\phi_{,\lambda}, \tag{65}$$

so that equation (59) can be automatically satisfied (i.e. $\phi_{,12} - \phi_{,21} = 0$). From (65), the linearized Euler equation (equation (58)) can be rewritten as

$$\dot{p}_{,i} = 2\mu\varepsilon_{\lambda i}\phi_{,\lambda AA} - E\phi_{,211}\delta_{i1} - C\varepsilon_{\lambda i}\phi_{,\lambda 1111}. \tag{66}$$

By utilizing the compatibility condition for $\dot{p}_{,i}$ (i.e. $\dot{p}_{,ij} = \dot{p}_{,ji}$), we obtain the following partial differential equation:

$$\Delta[\Delta\phi - \frac{\alpha}{2}\phi_{,1111}] + \frac{\alpha}{2}\phi_{,1122} = 0, \quad \text{where} \quad \beta = \frac{E}{\mu}, \alpha = \frac{C}{\mu} > 0 \text{ (material constants).} \tag{67}$$

We note here that the solution of the above equation can not be accommodated by conventional methods such as the separation of variables method, Fourier transform and polynomial solutions. In view of the solution of the modified Helmholtz equation, we assume that ϕ takes the form of $\phi = X(x)\sin(my)$ and obtain

$$\phi(x,y) = \sum_{m=1}^{\infty}[\{A_m e^{xT} + B_m e^{-xT} + e^{a_m x}(C_m \cos b_m x + D_m \sin b_m x) +$$
$$e^{-a_m x}(E_m \cos b_m x + F_m \sin b_m x)\} \times (\sin my)], \tag{68}$$

where

$$a_m = \sqrt{\frac{\sqrt{\left(\frac{\sqrt{3}}{2}\left(\frac{P}{Q}+Q\right)\right)^2 + \left(-\frac{Q}{2}+\frac{P}{2Q}-\frac{B}{3A}\right)^2} + \left(-\frac{Q}{2}+\frac{P}{2Q}-\frac{B}{3A}\right)}{2}},$$

$$b_m = \sqrt{\frac{\sqrt{\left(\frac{\sqrt{3}}{2}\left(\frac{P}{Q}+Q\right)\right)^2 + \left(-\frac{Q}{2}+\frac{P}{2Q}-\frac{B}{3A}\right)^2} - \left(-\frac{Q}{2}+\frac{P}{2Q}-\frac{B}{3A}\right)}{2}},$$

$$m = \frac{\pi n}{2d}, \quad A = \frac{\alpha}{2}, \quad B = \left(1+\frac{\alpha}{2}m^2\right), \quad D = -m^2(2+\frac{\beta}{2}),$$

$$Q = \left(\left(\left(\frac{D}{3A}-\frac{B^2}{9A^2}\right)^3 + \left(\frac{B^3}{27A^3}+\frac{m^4}{2A}-\frac{B.D}{6A^2}\right)^2\right)^{\frac{1}{2}} - \frac{B^3}{27A^3} - \frac{m^4}{2A} + \frac{BD}{6A^2}\right)^{\frac{1}{3}}$$

and $P = \frac{D}{3A} - \frac{B^2}{9A^2}$, $T = \left(Q - \frac{P}{Q} - \frac{B}{3A}\right)^{\frac{1}{2}}$. The unknown constant real numbers A_m, B_m, C_m, D_m, E_m and F_m can be completely determined by imposing the admissible boundary conditions given in equations (61) to (64). The corresponding stress and displacement fields can be also determined through equations (62), (65) and (66) (e.g. $u_1 = -\phi_{,2}$, $u_2 = \phi_{,1}$, etc.). For example, in the case of symmetric bending (see Figure 1), we have
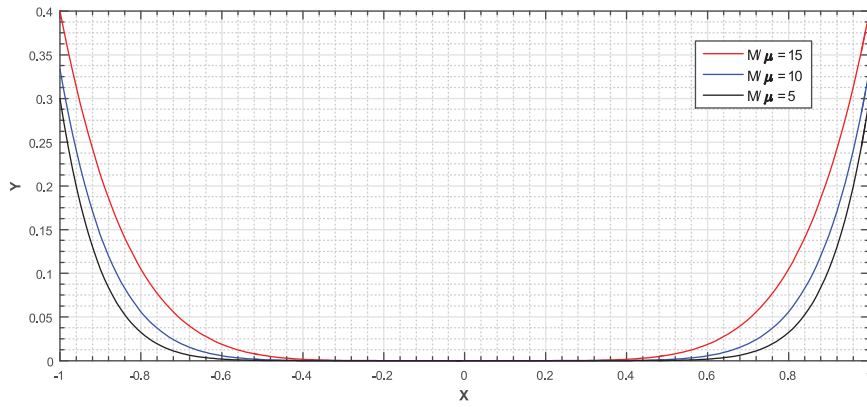
$$\dot{\mathbf{m}} = \dot{m}_1\mathbf{e}_1 + \dot{m}_2\mathbf{e}_2, \quad \dot{m}_1 = 5 \approx \sum_{n=1}^{30} \frac{20}{\pi n}(-1)^{\frac{n-1}{2}}\cos(\frac{\pi n}{2d})y\mathbf{e}_1, \quad \dot{m}_2 = 0, \tag{69}$$
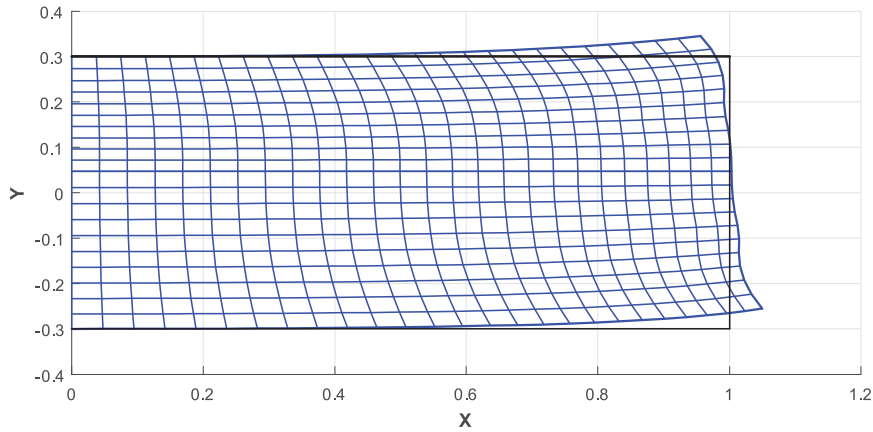
and

$$\mathbf{D} = D_1\mathbf{E}_1 + D_2\mathbf{E}_2, \quad D_1 = 1, \quad D_2 = 0. \tag{70}$$
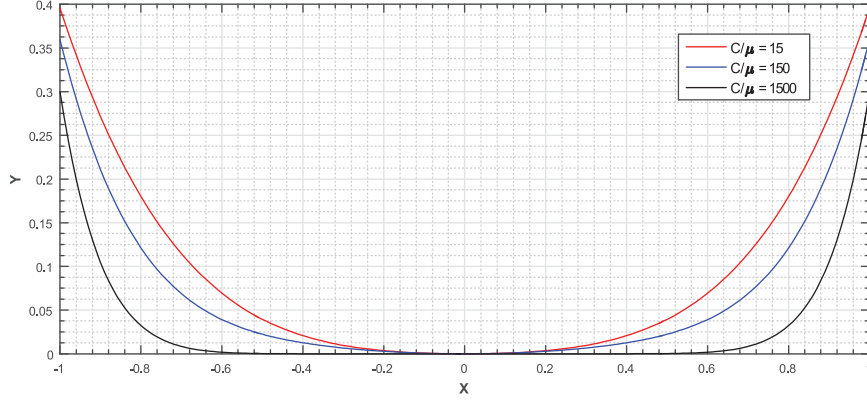
Figure 9. Deformation profiles with respect to C/μ when $M/\mu = 5$ and $E/\mu = 50$.

**Figure 10.** Deformation profiles with respect to M/μ when $C/\mu = 150$ and $E/\mu = 50$.

Figure 11. Deformed configuration of the fiber composite when $C/\mu = 150$, $E/\mu = 100$ and $M/\mu = 5$.

Thus

$$\dot{m}_1 = Cu_{1,11} = -\phi_{,211} = \sum_{n=1}^{30} \frac{20}{\pi n}(-1)^{(n-1)/2} \cos\left(\frac{\pi n}{2d}\right) y$$

$$\dot{m}_2 = Cu_{2,11} = \phi_{,111} = 0, \tag{71}$$

and similarly for the symmetry (about the y-axis) and continuity conditions. Here, the applied moment is approximated using Fourier series (see equation (69)) indicating fast convergence (within 30 iterations) and
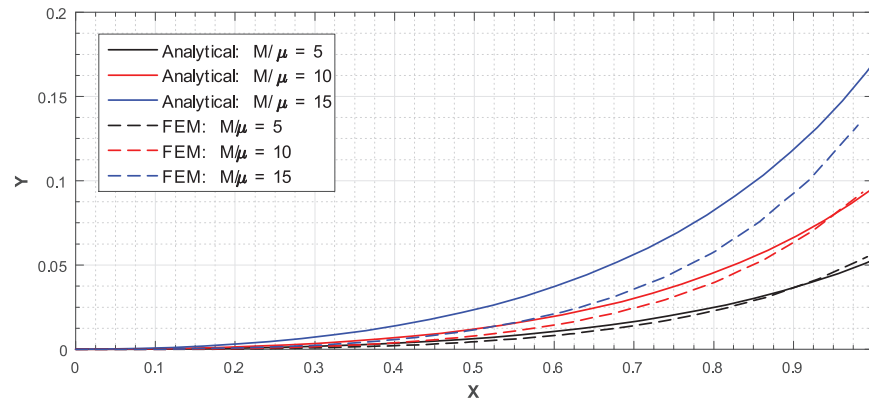
Figure 12. Solutions of the bending problem with $C/\mu = 150$ and $E/\mu = 100$. Nonlinear solution: dashed line; linear solution: solid line.

the corresponding results are summarized in Figures 9 to 12. Despite the inherent complexities of the presented PDE, the solution demonstrates reasonable deformation profiles for the domain of interest with sufficient sensitivities to the parameters C, μ, E and M (see Figures 9 and 10). In addition, the analytical (linear) solution shows good agreement with the non-linear solution (finite element method) for the small deformation regime, while larger values of M induce a significant discrepancy between the linear and non-linear solutions (see Figure 12).

Acknowledgements

Funding

References

[1]   Adkins, JE. Finite plane deformation of thin elastic sheet reinforced with inextensible cords. *Phil Trans R Soc Ser A* 1956; 249: 125–150.
[2]   Ericksen, JL, and Rivlin, RS. Large elastic deformations of homogeneous anisotropic materials. *J Rat Mech Anal* 1954; 3: 281–301.
[3]   Spencer, AJM. *Deformations of fibre-reinforced materials*. Oxford: Oxford University Press, 1972.
[4]   Pipkin, AC. Stress analysis for fiber-reinforced materials. *Adv Appl Mech* 1979; 19: 1–51.
[5]   Mulhern, JF, Rogers, TG and Spencer, AJM. A continuum model for fibre-reinforced plastic materials. *Proc R Soc Lond A* 1967; 301: 473–492.
[6]   Dow, NF (1963) Study of stresses near a discontinuity in a filament-reinforced composite material. *Gen Elect Co* Report number R63-SD-61.
[7]   Mulhern, JF, Rogers, TG and Spencer, AJM. A continuum theory of a plastic-elastic fibre-reinforced material. *Int J Eng Sci* 1969; 7: 129–152.
[8]   Pipkin, AC, and Rogers, TG. Plane deformations of incompressible fiber-reinforced materials. *ASME J Appl Mech* 1971; 38(8): 634–640.
[9]   Spencer, AJM and Soldatos, KP. Finite deformations of fibre-reinforced elastic solids with fibre bending stiffness. *Int J Non-Lin Mech* 2007; 42: 355–368.
[10]   Toupin, RA. Theories of elasticity with couple stress. *Arch Rat Mech Anal* 1964; 17: 85–112.
[11]   Mindlin, RD, and Tiersten, HF. Effects of couple-stresses in linear elasticity. *Arch Rat Mech Anal* 1962; 11: 415–448.
[12]   Koiter, WT. Couple-stresses in the theory of elasticity. *P K Ned Akad Wetensc B* 1964; 67: 17–44.
[13]   Steigmann, DJ. Theory of elastic solids reinforced with fibers resistant to extension, flexure and twist. *Int J Non-Lin Mech* 2012; 47: 743–742.

[14] Truesdell, C, and Noll, W. The non-linear field theories of mechanics. In: Flugge, S (ed.) *Handbuch der Physik*, vol. III/3. Berlin: Springer, 1965.

[15] Reissner, E. A further note on finite-strain force and moment stress elasticity. *Z Angew Math Phys* 1987; 38: 665–673.

[16] Pietraszkiewicz, W, and Eremeyev, VA. On natural strain measures of the non-linear micropolar continuum. *Int J Solid Struct* 2009; 46: 774–787.

[17] Germain, P. The method of virtual power in continuum mechanics, part 2: Microstructure. *SIAM J Appl Math* 1973; 25: 556–575.

Appendix 1: Finite element analysis of the fourth-order coupled PDE

It is not trivial to demonstrate numerical analysis procedures for coupled PDE systems, especially for those with high-order terms. For pre-processing, equation (36) can be expressed as

$$
\mu\left(R + \chi_{1,22}\right) - A\chi_{2,2} + B\chi_{2,1} - CR_{,11} - \frac{1}{2}EQ + \frac{1}{2}E(3Q\chi_{1,1}\chi_{1,1} + Q\chi_{2,1}\chi_{2,1} + 2R\chi_{1,1}\chi_{2,1}) = 0,
$$
$$
\mu\left(Q + \chi_{2,22}\right) + A\chi_{1,2} - B\chi_{1,1} - CQ_{,11} - \frac{1}{2}ER + \frac{1}{2}E(3R\chi_{2,1}\chi_{2,1} + R\chi_{1,1}\chi_{1,1} + 2Q\chi_{2,1}\chi_{1,1}) = 0,
$$
$$
C\chi_{2,2} - D\chi_{1,2} - 1 = 0,
$$
$$
Q - \chi_{1,11} = 0,
$$
$$
R - \chi_{2,11} = 0,
$$
$$
C - \chi_{1,1} = 0,
$$
$$
D - \chi_{2,1} = 0,
$$
$$
A - \mu(\chi_{1,11} + \chi_{1,22}) - CR_{,11} = 0,
$$
$$
B - \mu(\chi_{2,11} + \chi_{2,22}) - CQ_{,11} = 0,
\tag{72}
$$

where $Q = \chi_{1,11}$, $R = \chi_{2,11}$, $C = \chi_{1,1}$, and $D = \chi_{2,1}$. The non-linear terms in the above can be replaced by

$$
-A\chi_{2,2} + B\chi_{2,1} \implies -A_0\chi_{2,2} + B_0\chi_{2,1}
$$
$$
A\chi_{1,2} - B\chi_{1,1} \implies A_0\chi_{1,2} - B_0\chi_{1,1}
$$
$$
C\chi_{2,2} - D\chi_{2,1} \implies C_0\chi_{2,2} - D_0\chi_{2,1},
\tag{73}
$$

where the values of A, B and C continue to be refreshed based on their previous estimations (A_o, B_o and C_o) as iteration progresses. Therefore, the weak form of (72) is obtained by

$$
0 = \int_{\Omega} (\mu w_1 R - \mu w_{1,2}\chi_{1,2} - w_1 A_0\chi_{2,2} + w_1 B_0\chi_{2,1} + Cw_{1,1}R_{,1} - \frac{1}{2}Ew_1 Q
$$
$$
+ \frac{1}{2}Ew_1(3QC_0^2 + QD_0^2 + 2RC_0D_0))\,d\Omega + \int_{\partial\Gamma} (\mu w_1\chi_{1,2})N\,d\Gamma - \int_{\partial\Gamma} (Cw_1 R_{,1})N\,d\Gamma,
$$
$$
0 = \int_{\Omega} (\mu w_2 Q - \mu w_{2,2}\chi_{2,2} + + w_2 A_0\chi_{1,2} - w_2 B_0\chi_{1,1} + Cw_{2,1}Q_{,1} - \frac{1}{2}Ew_2 R
$$
$$
+ \frac{1}{2}w_2 E(3RD_0^2 + RC_0^2 + 2QD_0C_0))\,d\Omega + \int_{\partial\Gamma} (\mu w_2\chi_{2,2})N\,d\Gamma - \int_{\partial\Gamma} (Cw_2 Q_{,1})N\,d\Gamma,
$$
$$
0 = \int_{\Omega} C_0 w_3\chi_{2,2} - D_0 w_3\chi_{1,2} - w_3)\,d\Omega,
$$
$$
0 = \int_{\Omega} (w_4 Q + w_{4,1}\chi_{1,1})\,d\Omega - \int_{\partial\Gamma} (w_4\chi_{1,1})N\,d\Gamma,
$$

$$0 = \int_{\Omega} (w_5 R + w_{5,1} \chi_{2,1}) \, d\Omega - \int_{\partial \Gamma} (w_5 \chi_{2,1}) N \, d\Gamma,$$

$$0 = \int_{\Omega} (w_6 C - w_6 \chi_{1,1}) \, d\Omega,$$

$$0 = \int_{\Omega} (w_7 D - w_7 \chi_{2,1}) \, d\Omega,$$

$$0 = \int_{\Omega} (w_8 A + \mu w_{8,1} \chi_{1,1} - \mu w_{8,2} \chi_{1,2} + C w_{8,1} R_{,1}) \, d\Omega - \int_{\partial \Gamma} (\mu w_8 \chi_{1,1}) N \, d\Gamma$$

$$+ \int_{\partial \Gamma} (\mu w_8 \chi_{1,2}) N \, d\Gamma - \int_{\partial \Gamma} (C w_8 R_{,1}) n \, d\Gamma,$$

$$0 = \int_{\Omega} (w_9 B + \mu w_{9,1} \chi_{2,1} - \mu w_{9,2} \chi_{2,2} + C w_{9,1} Q_{,1}) \, d\Omega - \int_{\partial \Gamma} (\mu w_9 \chi_{2,1}) N \, d\Gamma$$

$$+ \int_{\partial \Gamma} (\mu w_9 \chi_{2,2}) N \, d\Gamma - \int_{\partial \Gamma} (C w_9 Q_{,1}) N \, d\Gamma, \tag{74}$$

where the unknowns χ_1, χ_2, Q_1, R_1, A and B can be written in the form of a Lagrangian polynomial such that $(*) = \sum_{j=1}^{n} [(*)_j \Psi_j(x, y)]$. Further, Ω, $\partial \Gamma$ and $\mathbf{N}$ are the domain of interest, the associated boundary, and the rightward unit normal to the boundary $\partial \Gamma$ in the sense of the Green–Stokes theorem, respectively. The corresponding test function w is given by

$$w = \sum w_i \Psi_i(x, y), \tag{75}$$

where w_i is the weight of the test function and $\Psi_i(x, y)$ are the shape functions; $\Psi_1 = \frac{(x-c)(y-d)}{cd}$, $\Psi_2 = \frac{x(y-d)}{-cd}$, $\Psi_3 = \frac{xy}{cd}$ and $\Psi_4 = \frac{y(x-c)}{-cd}$. Here c and d are dimensions of the domain as illustrated in Figure 1. Using Lagrangian polynomial representation, the first equation of (74) can be rearranged as

$$0 = \sum \{ \int_{\Omega} (\mu \Psi_i \Psi_j + C \Psi_{i,1} \Psi_{j,1}) \, d\Omega \} R_j - \sum \{ \int_{\Omega} (\mu \Psi_{i,2} \Psi_{j,2}) \, d\Omega \} \chi_{1j}$$

$$- \sum \{ \int_{\Omega} (\Psi_i A_0 \Psi_{j,2} + \Psi_i B_0 \Psi_{j,1}) \, d\Omega \} \chi_{2j} + \sum \{ \int_{\Omega} -(\frac{1}{2} E \Psi_i + \frac{1}{2} E \Psi_i (3 C_0^2 + D_0^2) \, d\Omega \} Q_j$$

$$+ \sum \{ \int_{\Omega} \frac{1}{2} E \Psi_i (2 C_0 D_0)) \, d\Omega \} R_j + \int_{\partial \Gamma} (\mu \Psi_i \chi_{1,2}) N \, d\Gamma - \int_{\partial \Gamma} (C \Psi_i R_{,1}) N \, d\Gamma, \tag{76}$$

and similarly for the rest of the equations. Consequently, we obtain the following systems of equations:

$$\begin{bmatrix} [K^{11}] & [K^{12}] & [K^{13}] & [K^{14}] & [K^{15}] & [K^{16}] & [K^{17}] & [K^{18}] \\ [K^{21}] & [K^{22}] & [K^{23}] & [K^{24}] & [K^{25}] & [K^{26}] & [K^{27}] & [K^{28}] \\ [K^{31}] & [K^{32}] & [K^{33}] & [K^{34}] & [K^{35}] & [K^{36}] & [K^{37}] & [K^{38}] \\ [K^{41}] & [K^{42}] & [K^{43}] & [K^{44}] & [K^{45}] & [K^{46}] & [K^{47}] & [K^{48}] \\ [K^{51}] & [K^{52}] & [K^{53}] & [K^{54}] & [K^{55}] & [K^{56}] & [K^{57}] & [K^{58}] \\ [K^{61}] & [K^{62}] & [K^{63}] & [K^{64}] & [K^{65}] & [K^{66}] & [K^{67}] & [K^{68}] \\ [K^{71}] & [K^{72}] & [K^{73}] & [K^{74}] & [K^{75}] & [K^{76}] & [K^{77}] & [K^{78}] \\ [K^{81}] & [K^{82}] & [K^{83}] & [K^{84}] & [K^{85}] & [K^{86}] & [K^{87}] & [K^{88}] \\ [K^{91}] & [K^{92}] & [K^{93}] & [K^{94}] & [K^{95}] & [K^{96}] & [K^{97}] & [K^{98}] \end{bmatrix} \begin{bmatrix} \chi_1 \\ \chi_2 \\ Q \\ R \\ A \\ B \\ C \\ D \end{bmatrix} = \begin{bmatrix} \{F_1\} \\ \{F_2\} \\ \{F_3\} \\ \{F_4\} \\ \{F_5\} \\ \{F_6\} \\ \{F_7\} \\ \{F_8\} \\ \{F_9\} \end{bmatrix}, \tag{77}$$

where the expressions of $[K^{ij}]$ and F_i can be obtained via the standard finite element analysis procedures, for example

$$[K^{11}] = \int_{\Omega} (\mu \Psi_{i,2} \Psi_{j,2}) \, d\Omega,$$

and

$$\{F_1\} = - \int_{\partial \Gamma} (\mu \Psi_i \chi_{1,2}) N \, d\Gamma + \int_{\partial \Gamma} (C \Psi_i R_{,1}) N \, d\Gamma.$$